Spectroscopic Characterization of Gold Nanoparticles Passivated by Mercaptopyridine and Mercaptopyrimidine Derivatives

Hao-Li Zhang,[†] Stephen D. Evans,*[,†] J. R. Henderson,[†] Robert E. Miles,[‡] and Tiehan Shen[§]

Department of Physics and Astronomy, University of Leeds, Leeds, LS2 9JT, U.K., School of Electronic and Electrical Engineering, University of Leeds, Leeds, LS2 9JT, U.K., and Joule Physics Laboratory, Institute for Materials Research, University of Salford, Salford, Greater Manchester, M5 4WT, U.K.

Received: February 25, 2003

A series of gold nanoparticles stabilized by the adsorption of heterocyclic mercaptan derivatives, including 2-mercaptopyridine (2MPy), 2-mercaptopyrimidine (2MPm) and 4-mercaptopyridine (4MPy), were synthesized and characterized by TEM, FTIR, UV−vis, and XPS. The adsorption of 2MPy molecules led to the most stable and uniform nanoparticles. In contrast, the 4MPy-coated nanoparticles showed a strong tendency to form 3D aggregates, which is attributed to cross linking between sulfur groups on neighboring particles. FTIR and UV−vis spectroscopy were employed to study the chemical conformation of the heterocyclic molecules on the gold surface. Significant differences between the IR spectra of the functionalized nanoparticles and the free mercaptan molecules were observed. Interpretations of these IR spectra were achieved with the aid of ab initio calculations. We found that the "thione form" is predominant when the molecules are either in a polycrystalline state or in methanol solution; however, they are stabilized in the "thiol-like form" when adsorbed on the particles. The XPS spectra of the 2MPy nanoparticles showed narrow peaks with the expected peak position. In contrast, the peaks in the spectra of the 2MPm- and 4MPy-passivated nanoparticles were strongly shifted. Oxidization of the sulfur group was detected in the 4MPy-modified nanoparticles, indicating that some molecules were adsorbed onto the gold surface via their nitrogen groups.

Introduction

Gold nanoparticles stabilized by various mercaptan molecules have recently attracted great interest.[1−3] This is partially because of the unique chemical, physical, and electronic properties associated with their reduced dimensions as well as their potential use in a diverse range of applications from electronic nanodevices and chemical sensors[4,5] to biological tagging.[6,7] Previous studies have shown that coating such nanoparticles with alkanethiols helps to promote solubility in nonaqueous media as well as enhances their stability in both solution and in dry form. More recently, however, the stabilizing ligand has been extended to include a wide range of molecules containing various functional groups.[8−10] By controlling the conditions used in the synthesis of nanoparticles, one is able to tailor the properties of the passivated nanoparticles. For example, some size control can be achieved by controlling the relative amount of the reactants (i.e., the gold-to-thiol ratio).[11−13] Furthermore, by using different stabilizing ligands, one can make nanoparticles that are soluble in different media.[14−16] Such functionalized nanoparticles can be used as basic building blocks for constructing 2D or 3D structures that have the potential to be new nanoscale electronic or electro-optic devices.[4,17,18]

Previously, we studied a series of gold nanoparticles stabilized with small bifunctional aromatic molecules[19] and demonstrated that their chemical and physical behavior is dominated by the functional groups exposed to the ambient. In this work, we report our studies on nanoparticles passivated with small heterocyclic mercaptan derivatives: 2-mercaptopyridine (2MPy), 4-mercaptopyridine (4MPy), and 2-mercaptopyrimidine (2MPm). One potential use of these molecules as passivating reagents is to obtain positively charged nanoparticles that might be used for the formation of 3D self-assembled nanostructures or for use in biological nanotagging. Furthermore, the feasibility of using heterocyclic molecules as passivating reagents is of fundamental interest because of the possible thione−thiol tautomerism of the mercaptopyridine and mercaptopyrimidine molecules.[20,21] Indeed, the thione form can often be the preferable structure of these molecules in the crystalline state[23] and even in solution (Scheme 1).

The adsorption of 2MPy, 4MPy, and 2MPm on planar noble-metal surfaces has attracted increasing attention in recent years.[23,24] One of the reasons for this interest is that under certain conditions these molecules significantly enhance electron transfer between proteins (e.g., cytochrome C) and an electrode.[25,26] To date, most of the investigations suggest that 2MPy, 4MPy, and 2MPm are adsorbed on metal surfaces by the sulfur group. However, it has also been suggested that the mercaptopyridine molecules might bind to gold through its nitrogen atom.[27] Moreover, recent STM work has suggested that 4MPy forms a disulfide dimer when bonding to gold,[28] whereas the 2MPm forms hydrogen-bonded dimers on gold.[29] These studies show that heterocyclic mercaptan derivatives such as 2MPy, 4MPy, and 2MPm molecules have distinct properties that can be remarkably different from those displayed by the normal aromatic thiols such as thiophenol. To understand how these molecules passivate metal nanoparticles is therefore an interesting issue. In this work, we perform systematic spectroscopic investigations of gold nanoparticles passivated by the above

* To whom correspondence should be addressed. E-mail: S.D.Evans@leeds.ac.uk. Phone: +44-113 343 3852. Fax: +44-113 343 1884.
[†] Department of Physics and Astronomy, University of Leeds.
[‡] School of Electronic and Electrical Engineering, University of Leeds.
[§] University of Salford.

10.1021/jp030297y CCC: $25.00
Published on Web 06/04/2003

SCHEME 1: Chemical Structures of the Molecules Studied in This Work and Their Possible Thione−Thiol Tautomerism[a]

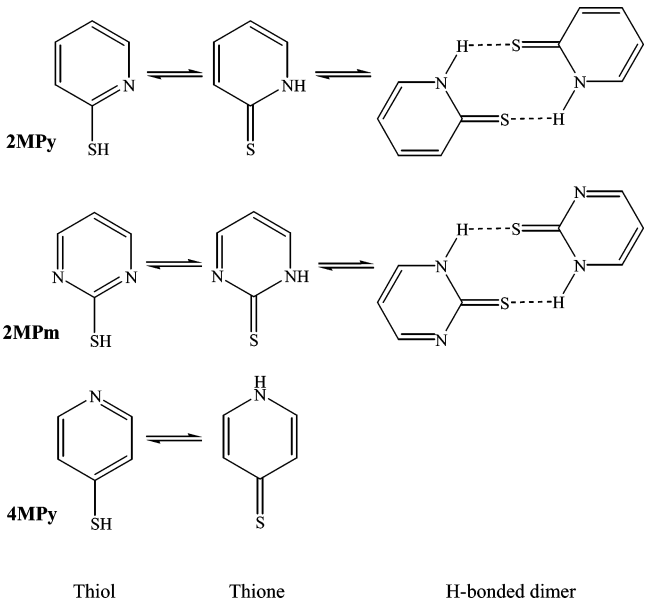

[a] 2MPy and 2MPm are able to form hydrogen-bonded dimers.

molecules to reveal the tautomeric form they adopt when adsorbed on the nanoparticle surface. We also provide an assignment of the vibrational modes of these three molecules when adsorbed on gold nanoparticles. This assignment will be important for further spectroscopic investigations (e.g., surface-enhanced Raman spectroscopic (SERS) studies).[30−32]

Experimental Section

Chemicals. Sodium borohydride (99%, Aldrich), hydrogen tetrachoroaurate(III) trihydrate, (99%, Aldrich), 2-mercaptopyridine (2MPy, 98%, Aldrich), 4-mercaptopyridine (4MPy, 95%, Aldrich), and 2-mercaptopyrimidine (2MPM, 98%, Aldrich) were used as received. Water (>18 MΩ) was obtained with a MilliQ water system. All other solvents were of HPLC purity and were used as received.

Synthesis. The synthesis of surface-functionalized gold nanoparticles follows a similar procedure for making gold nanoparticles modified with aromatic mercaptan molecules.[19] For example, 6 mL of 50 mM $HAuCl_4 \cdot 3H_2O$ methanol solution (0.3 mmol) was mixed with 0.067 g of 2MPy in 10 mL of methanol (0.6 mmol) at room temperature. Then a freshly made aqueous solution of $NaBH_4$ (3 mmol) was added slowly while the mixture was being vigorously stirred. There was an immediate color change of this solution from yellow to black in the flask. The solution was then left, at 20 °C while being continually stirred, for 3 h to achieve thermodynamic equilibrium. Afterward, the solvent was evaporated off under a steady stream of nitrogen. Finally, the product was washed with diethyl ether and water to remove the excess materials.

Transmission Electron Microscopy. Bright-field images were obtained using a Philips CM20 TEM operating at 200 kV. The samples were prepared by placing a dilute solution containing the nanoparticles on a carbon-coated copper grid (400 mesh) and allowing the solvent to evaporate. The nanoparticle size distributions were determined via a Kontron Electronik Image Analyzer using IBAS software version 2.5.

X-ray Photoelectron Spectroscopy. High-resolution XPS measurements were made using the Scienta ESCA-300 instrument at Daresbury Laboratories, Warrington, U.K. A monochromated Al Kα X-ray source at 1486.7 eV was used. C 1s, N 1s, O 1s, Au 4f, and S 2p levels were recorded at an electron take-off angle of 90°. The base pressure in the sample chamber was $<10^{-9}$ mbar. The power level used was 2.8 kW for all samples. The analyzer slit width and pass energy were 1.9 mm and 150 eV, respectively, and the system was calibrated with respect to the Ag 3d peak from a standard sample. The system resolution under the above conditions, as determined from the Ag 3d peak, is better than 0.7 eV.

UV−Visible Spectroscopy. UV−vis spectra were obtained using a Shimadzu UV-2101PC UV−vis scanning spectrophotometer. Solution spectra were obtained by measuring the absorption of dilute solutions in a quartz cell with a path length of 1 cm; the solvent used was methanol.

Fourier Transform Infrared Spectroscopy. Transmission spectra for the nanoparticles and the aromatic heterocyclic mercaptans were obtained by forming thin, transparent KBr pellets containing the materials of interest. The KBr mixtures were placed on a vacuum line overnight before pellet formation, and then the pellets were again placed on a vacuum line before use. The transmission spectra were obtained, after purging in dry air, and were background corrected using a reference "blank" KBr pellet. Spectra were obtained for 200 scans at a resolution of 2 cm^{-1}.

The ab initio calculations for the frequency and intensities of vibrational modes were performed with the Gaussian 98 program package using a restricted Hartree−Fock method with the 6-31G(d, p) basis set.[33] The calculated frequencies were rescaled using a calibration factor of 0.8929.[34] The spectral envelopes have been constructed by convoluting the bare spectrum with Gaussian peaks of fwhm = 5 cm^{-1}. Infrared spectra of molecules in the thiol and thione forms were calculated.

Results and Discussion

Size Distribution and Stability. All nanoparticles obtained from the one-phase synthesis were dark brown in color when freshly made. The nanoparticles were not soluble in nonpolar organic solvents such as diethyl ether, chloroform, and toluene but were soluble in polar solvents such as methanol, ethanol, and acetone. However, they exhibit marked differences in stability. For instance, the 2MPy-functionalized nanoparticles are stable when dispersed in methanol. The solution is a "clear" dark-brown color and remains transparent even after being left at room temperature for several months, showing no tendency to agglomerate or precipitate. Solutions of the 2MPm-modified nanoparticles, however, turn from dark brown to blue in a period of 2 to 3 days, indicating the formation of large aggregates. Finally, the 4MPy-passivated gold nanoparticles display such a strong tendency to form aggregates that they start to precipitate during the synthesis. Indeed, in only a few hours after synthesis, all of the suspended material had precipitated from the solution, giving a black flocculate.

The size distribution of the nanoparticles was characterized with electron microscopy. Representative TEM micrographs of the different nanoparticles are shown in Figure 1. The 2PMy-functionalized nanoparticles were approximately spherical in shape, had a mean diameter of 4.8 ± 0.8 nm (Figure 1a), and were the smallest of the three sample types. The 2PMm nanoparticles have an average diameter of 8.6 ± 1.6 nm and displayed a propensity to form 2D structures on the TEM grid upon solvent evaporation (Figure 1b). The average size of 4MPy nanoparticles is estimated to be 9.8 ± 2.8 nm (Figure 1c). Following solvent evaporation, these nanoparticles form ir-

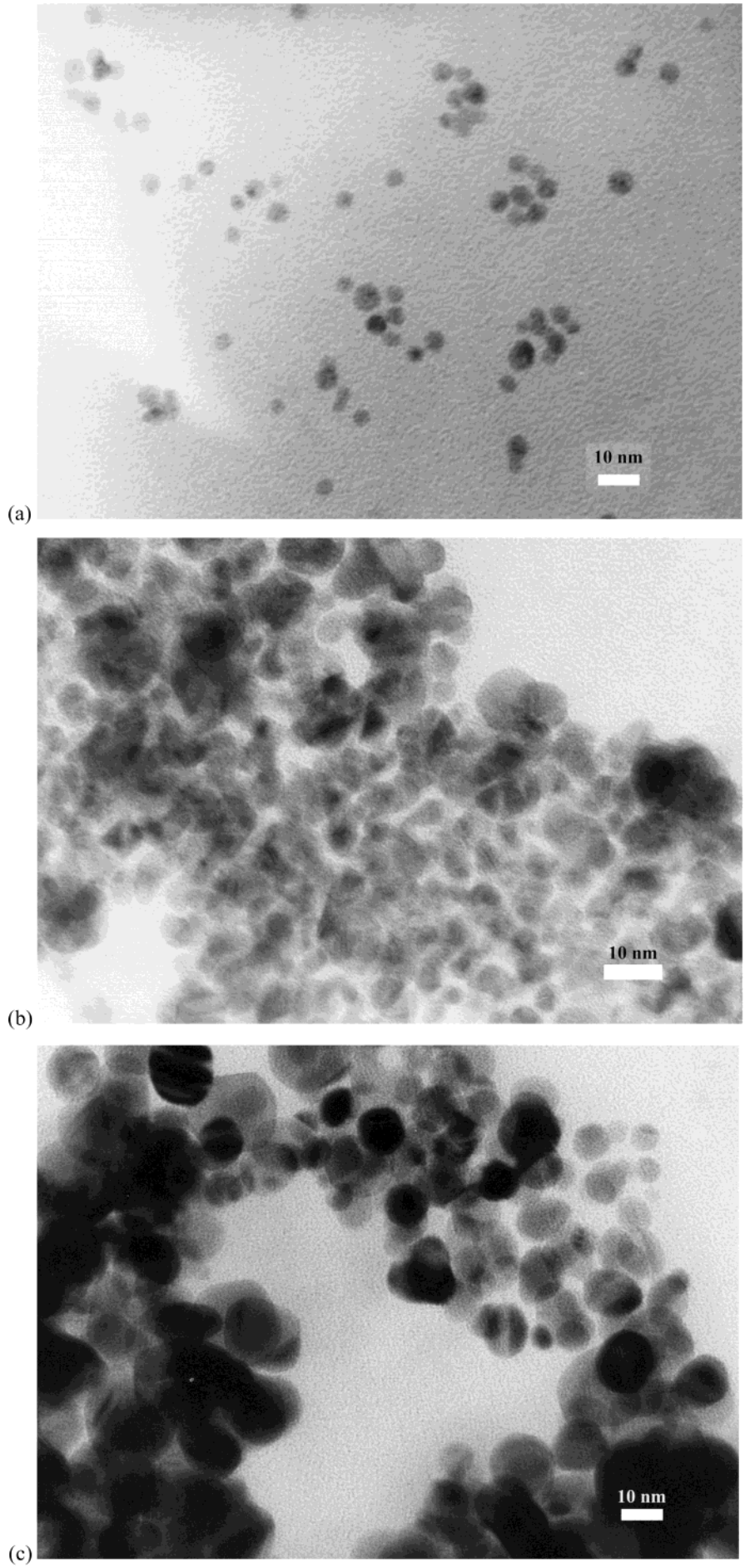

Figure 1. Representative TEM images of the nanoparticles passivated by (a) 2MPy, (b) 2MPm, and (c) 4Mpy.

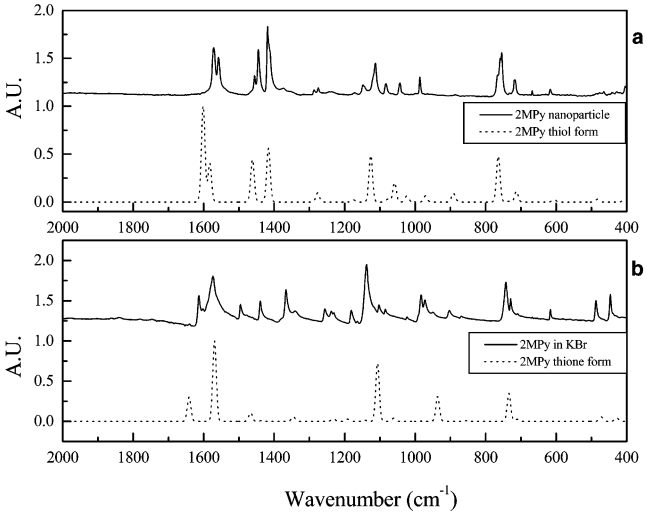

Figure 2. IR spectra of (a) 2MPy-passivated gold nanoparticles dispersed in KBr pellets and (b) 2MPy molecules in a polycrystalline KBr pellet. The dotted curves are the calculated spectra of 2MPy in the (a) thiol and (b) thione forms.

regular 3D aggregates on the TEM grid, consistent with the observation that they tend to agglomerate and precipitate out of solution. A plausible explanation for this result is that the 4MPy molecule has two heteroatoms, S and N, on opposite sides of the molecule. Although it is normally assumed that the sulfur group preferentially adsorbs at the gold surface, it is possible that the 4MPy molecule could bind via the nitrogen.[27] In this case, the free sulfur group will be exposed at the surface; consequently, these nanoparticles could cross link with others via the formation of disulfide bonds between the sulfur groups on neighboring particles. Such binding between particles would be expected to give rise to irreversible aggregation.

FTIR. It is well known that aromatic heterocyclic molecules bearing a mobile H atom undergo rapid and facile tautomeric transformations in solution. It has also been reported that, under ambient conditions, the pyridine or pyrimidine derivatives substituted at the 2 or 4 position by potentially tautomeric groups, SH in this case, exist as the thione form rather than the thiol when in polar solution.[21] Because the nanoparticles were prepared under highly polar conditions, the molecules adsorbed onto the gold surfaces come from a thione-rich solution. Thus, the first question to be addressed is that regarding the configuration that these molecules adopt on the nanoparticles.

An IR transmission spectrum of the 2MPy-passivated gold nanoparticles dispersed in a KBr pellet is shown in Figure 2. For simplicity, only the spectra in the region from 2000−400 cm^{-1} are given, which are mainly associated with ring-stretching and hydrogen bending modes. For comparison, a transmission spectrum of the 2MPy molecules in KBr is also given. Significant differences between these two classes of spectra can be seen, indicating that the molecules experience a structural change on adsorption. It is known that in the polycrystalline state (in polycrystalline KBr pellets) 2MPy exists in its thione form as a hydrogen-bonded dimer[22] (Scheme 1). However, if the 2MPy is adsorbed onto gold through the sulfur group, then such hydrogen-bonded dimers cannot be formed on the nanoparticle, hence the molecules should adopt a configuration more like that of a thiol form. Unfortunately, it is difficult to obtain a spectrum of the thiol form, vide infra, so to aid in the interpretation of the IR spectra, ab initio calculations of the 2MPy in both the thione and thiol forms were performed (Figure 2). Similar calculations have been employed in previous investigations of the vibrational properties of pyridine and pyrimidine derivatives and have been shown to give reasonable consistency with the experimental spectra.[37−39]

The frequencies as well as the relative intensities of different vibrational modes calculated from the ab initio computation are also shown in Figure 2 (dashed lines), from which one can see that the calculated spectrum of the 2MPy thione form shows a pattern similar to the transmission spectrum of the 2MPy molecule in KBr. The ring stretching combined with the hydrogen in-plane wagging modes is predicted to give rise to a medium-intensity peak around 1641 cm^{-1}, a strong peak at 1569 cm^{-1}, and a relatively weak peak near 1466 cm^{-1} compared with 1613, 1574, and 1496 cm^{-1}, respectively, for the experimentally obtained 2MPy spectrum. Two strong peaks are predicted near 1106 and 936 cm^{-1}, which are associated with the hydrogen in-plane rocking, and are seen experimentally at 1138 and 984 cm^{-1}, respectively. Finally, hydrogen out-of-plane bending is predicted to be around 753 cm^{-1} but is actually observed at 743 cm^{-1}. Although it is evident that the calculated frequencies of the thione form are different from those that are observed, there is a clear correlation between the two, and the difference probably reflects the difference between the model and the real environments that the molecules are in. For instance, computation does not take into account intermolecular interactions because the frequencies calculated here correspond to the molecule in the gas phase. The molecular interactions in the crystal could easily shift the positions of the peaks, especially if hydrogen bonding is present. Another contribution to the difference may come from the imperfection of the basis set used in the theoretical calculations. In summary, the differences between the calculated spectrum of 2MPy in its thione forms and the peaks observed in the 2MPy transmission spectrum are to be expected and do not affect the assignment of the significant vibrational modes. From Figure 2, it is also evident that the calculated thiol spectrum shows a high degree of similarity with the spectrum of the 2MPy-passivated nanoparticles. This implies that the 2MPy species adsorbed to the nanoparticles are in a configuration similar to that of the thiol form. The reasonable agreement between the calculated and the observed spectra permits the assignment of the vibrational modes seen in the experimental spectra (Table 1).

The IR spectra of polycrystalline 2MPm- and 2MPm-passivated gold nanoparticles dispersed in KBr pellets and the calculated thione and thiol form spectra are presented in Figure 3. The assignments to the vibrational modes are listed in Table 2. Once again, the spectrum of the polycrystalline sample shows a similarity to the calculated thione spectrum. It can be seen that the frequencies estimated from ab initio computation are slightly shifted with respect to the measured ones because of intermolecular interactions. For example, the combination of the ring-stretching mode, 8b, with the N−H in-plane bending mode was predicted to occur at 1564 cm^{-1} but was actually observed at 1572 cm^{-1}, with its intensity being overestimated by the calculation. This discrepancy could be attributed to the presence of hydrogen bonding. In a previous investigation of 2MPm,[23] we have indicated that the 2MPm molecule exists as 2(1H)-pyrimidine-thione in the solid state (Scheme 1), but when adsorbed onto planar gold, it changes from thione to the thiolate (R−S−Au) form. In summary, Figure 3 shows that the IR spectrum from 2MPm adsorbed on gold nanoparticles is remarkably different from the polycrystalline spectrum, and it is notable that the spectrum of the nanoparticle sample is almost identical to the spectrum of 2MPm when formed as self-assembled monolayers (SAMs) on planar gold.[23] This latter spectrum is what would be expected for the thiolate form and

TABLE 1: Vibrational Assignment of the IR Spectra of 2MPy Molecules and 2MPy-Passivated Gold Nanoparticles Dispersed in KBr Pellets[a]

vibrational modes	2MPy in KBr	thione form (ab initio)	vibrational modes	2MPy nanoparticle	thiol form (ab initio)
8b	1613	1641	8b	1572	1601
8a, N−H bending	1574	1569	8b, S−H bending	1558	1582
19a, N−H bending	1496	1467	14	1445	1461
3	1367	1345	19b	1419	1416
18b	1138	1106	9a	1113	1125
15,1	984	936		1044	1058
11, N−H op. bending	743	733	10b	754	764

[a] Calculated spectra of gas -phase 2MPy in thione and the thiol form are also given for comparison. The specification of the vibrational modes is taken from the normal mode assignment of benzene.[35] All of the frequencies are in wavenumbers. op. denotes out of plane.

TABLE 2: Vibrational Assignment of the IR Spectra of 2MPm Molecules and 2MPy-Passivated Gold Nanoparticles Dispersed in KBr Pellets[a]

vibrational modes	2MPm in KBr	thione form (ab initio)	vibrational modes	2MPm nanoparticle	thiol form (ab initio)
8b	1608	1647	8a	1562	1601
8b, N−H bending	1572	1564	8b	1543	1582
19b, N−H bending	1493	1460	19a	1374	1461
3	1331	1334	19b	1173	1416
ring ip. deformation	1181	1176			
9b,3	983	992			
4	738	729	17b, 4	765	1125

[a] Calculated spectra of gas-phase 2MPy in thione and the thiol form are also given for comparison. ip. denotes in plane.

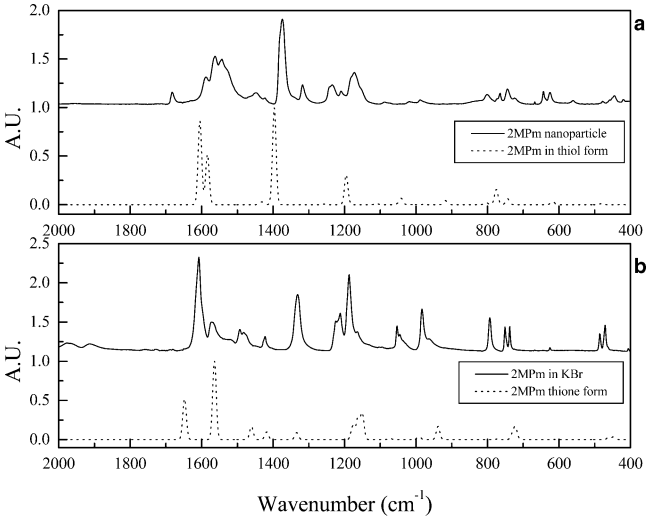

Figure 3. IR spectra of (a) 2MPm-passivated gold nanoparticles dispersed in KBr pellets and (b) 2MPm molecules in a polycrystalline KBr pellet. The dotted curves are the calculated spectra of 2MPm in the (a) thiol and (b) thione forms.

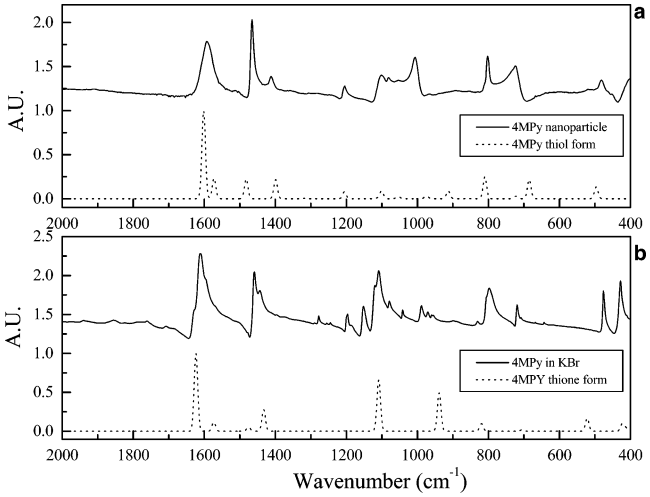

Figure 4. IR spectra of the (a) 4MPy-passivated gold nanoparticles dispersed in KBr pellets and (b) 4MPy molecules in a polycrystalline KBr pellet. The dotted curves are the calculated spectra of 4MPy in the (a) thiol and (b) thione forms.

strongly suggests that the 2MPm molecules are covalently bonded to the gold core through the formation of a sulfur−gold bond.

It is worth noting that the two small peaks located at 1682 and 1590 cm^{-1} in the observed nanoparticle spectrum are not predicted in the calculated thiol spectrum. These peaks are not seen in the 2MPm crystal spectrum and so cannot be due to the residual presence of the starting materials. Furthermore, no trace of these peaks was observed in the 2MPm SAMs,[23] indicating that 2MPm molecules adsorbed on the nanoparticles do not form exactly the same structure as those that are self-assembled on planar gold. The assignment of these two peaks is therefore not clear, but we note that the positions and the relative intensities of these peaks are similar to the ring-stretching modes at 1647 and 1564 cm^{-1}, expected for the non-hydrogen-bonded 2MPm molecules in the thione form. If these assignments are correct, then a small number of the 2MPm moieties remain in the thione form on the nanoparticles surface, but in contrast to the polycrystalline state, they are not hydrogen bonded.

Figure 4 presents the IR spectra of 4MPy molecules and 4MPy-passivated gold nanoparticles dispersed in KBr pellets as well as the calculated spectra of 4MPy in the thione and thiol forms, respectively. Similar to 2MPy and 2MPm, Figure 4 suggests that the polycrystalline 4MPy is in the thione form, and the nanoparticle spectrum implies that the molecules are attached to gold through Au−S bonds. Compared with the spectra in Figures 2 and 3, the ab initio calculation seems to give better predications because most of the calculated frequencies are within 10 wavenumbers of the observed peak positions (Table 3). This is presumably due to different intermolecular interactions in polycrystalline 4MPy compared with those in 2MPy and 2MPm. For example, 4MPy probably does not form dimers in the solid state.

UV−Visible Spectra. The UV−vis spectra of passivated nanoparticles dissolved in methanol solutions are recorded in

TABLE 3: Vibrational Assignment of the IR Spectra of 4MPy Molecules and 2MPy-Passivated Gold Nanoparticles Dispersed in KBr Pellets[a]

vibrational modes	4MPy in KBr	thione form (ab initio)	vibrational modes	4MPy nanoparticle	thiol form (ab initio)
8a	1612	1623	8b	1593	1601
	1459	1475	14	1466	1482
19a	1440	1433	19b	1412	1398
15, 12	1108	1109	9a, 12	1205	1205
15 + 8a	988	938	9a, 12	1101	1100
C−H op. bending	798	819	17b	802	810
			ip. ring deformation	724	685

[a] Calculated spectra of gas-phase 2MPy in thione and the thiol form are also given for comparison. ip. denotes in plane.

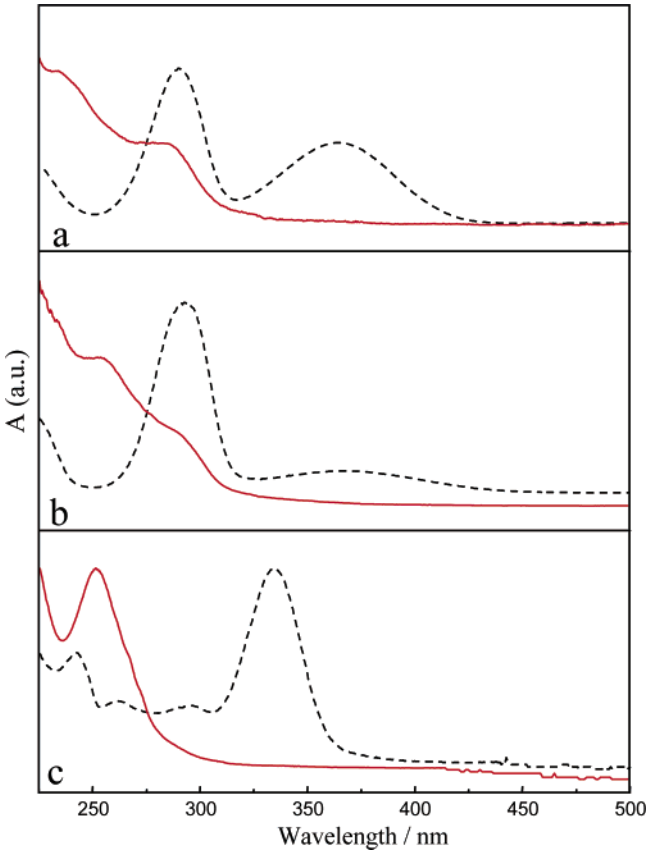

Figure 5. UV−vis spectra of (a) 2MPy-, (b) 2MPm-, and (c) 4MPy-passivated gold nanoparticles suspended in methanol. Spectra of the same compounds in methanol in the absence of gold are also shown (dashed lines).

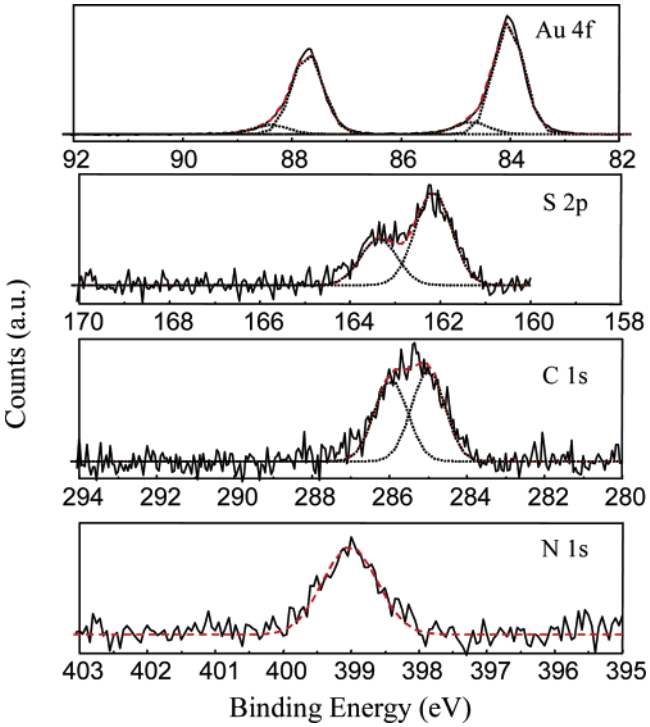

Figure 6. Au 4f, S 2p, C 1s, and N 1s regions of the XPS spectrum of 2MPy-passivated gold nanoparticles.

Figures 5 and 6. Figure 5 presents the spectral region between 220 and 500 nm. In this region, the absorption bands are attributed to electronic transitions in the organic moieties adsorbed on the nanoparticles. The spectra of solutions of the corresponding heterocyclic molecules in methanol are also presented for comparison. The spectrum of 2MPy in solution (Figure 5a) has two maxima at 360 and 284 nm that can be assigned to the n−π* and π−π* electronic transitions of the thione tautomer, respectively.[21] In contrast, the nanoparticles show no absorption at 360 nm but have two shoulders near 233 and 281 nm. The absorption at 233 nm has been previously reported to correspond to the spectrum of 2MPy molecules in the thiol form.[21] Hence, Figure 5a indicates that the 2MPy moieties adsorbed on the nanoparticles are in the thiol-like form, which is consistent with the observation from the IR spectra. The shoulder near 281 nm in the nanoparticle spectrum is possibly due to the π−π* transition of the thione tautomer[21] and may suggest that some of the 2MPy moieties remain in the thione form. Because the IR data (Figure 2) suggest that the 2MPy molecules adsorb through an Au−S bond and hence exist in a thiol-like form, the thione form observed in the UV−vis region of the nanoparticle spectrum is most likely due to effects from the solvent (i.e., adsorption/desorption equilibrium of the ligand molecules in solution).

The UV−vis spectra of the 2MPm nanoparticles also show significant differences from that of a 2MPm solution. In the solution spectrum, there is one peak at 287 nm and another broad and weaker absorption around 370 nm, corresponding to the thione-form tautomer. In the nanoparticle spectrum, there is a maximum absorption around 246 nm, indicating that the majority of the 2MPm molecules are in the thiol-like form. Furthermore, the shoulder in the nanoparticle spectrum at 283 nm suggests that a small number of 2MPm molecules are present in the solution, which might be attributed to the adsorption/desorption equilibrium in solution.

The spectrum of the 4MPy molecules in methanol (Figure 5c) has a strong peak at 337 nm and three small absorption bands between 230 nm to 300 nm corresponding to the thione-form tautomer. In the nanoparticle spectrum, only one peak around 250 nm is observed. The dramatic spectral difference in the nanoparticle spectrum compared with the spectrum of the 2MPy solution implies a structural change of the 4MPy molecules (i.e., from the thione tautomer in solution to a thiol-like form on the nanoparticles). However, the ligand in the

TABLE 4: XPS Binding-Energy Positions of Four Different Components Present with Nanoparticle Samples[a]

XPS bands	2MPy (eV)	2MPm (eV)	4MPy (eV)
Au 4f	84.0 (53.3), 84.7 (5.9) 87.7 (36.3), 88.4 (4.5)	84.2(52), 84.9(5.1) 87.8 (39.3), 88.6 (3.6)	84.1(46), 84.5(11) 87.8(36), 88.3 (7)
S $2p_{3/2}$	162.1(66.7)	161.8(21), 162.5 (33.2), 164.5(14)	161.5 (18.6), 162.5 (22.3), 164.5(18.9), 167.6 (6.8)
S $2p_{1/2}$	163.4 (33.3)	163.2 (10.8), 163.7 (16.1), 165.7 (5.4)	162.8 (9.3), 163.8 (11.2), 165.8 (9.5), 168.9 (3.4)
C 1s	285.0 (53.2), 286.0 (47)	284.8(31.5), 285.7(30.4), 286.6 (22.7), 287.6 (10.6) 288.6 (4.8)	284.9 (43.6), 285.7 (37.7), 286.5 (18.7)
N 1s	399.0	398.9 (44), 399.9 (34.5), 400.7(16.7), 401.7 (4.7)	398.8 (21.9), 399.6 (29.9), 400.6 (24.4), 401.5 (23.8)

[a] Relative amounts of atomic species are shown in brackets as percentages.

4MPy-coated nanoparticle, unlike those in the 2MPy and 2MPm nanoparticles, appears to be in the thiol-like form with no trace of the thione form. In summary, the UV−vis spectra indicate that for all three nanoparticle types the majority of the ligand molecules exist in a thiol-like form, which is consistent with the observations from the IR results.

The plasmon bands of the gold nanoparticles are observed in the range of 350−800 nm. The 2MPy and 2MPm nanoparticles show very broad absorption bands between 500 and 800 nm, probably indicative of a relatively broad size distribution of the particles and/or possibly indicating that there is some aggregation in solution. The 4MPy sample gave an extremely broad absorption band beginning at 500 nm and increasing into the red (not reaching a maximum before 800 nm). This abnormally broad absorption band can be attributed to the strong tendency of 4MPy nanoparticles to form 3D aggregates in solution.

X-ray Photoelectron Spectra (XPS). The XPS spectra from the nanoparticle films show the presence of both the Au core and the stabilizing ligand molecules. No trace of the starting materials was found in any of the spectra. Figure 6 shows the spectra of the 2MPy-modified gold nanoparticles. The Au $4f_{7/2}$ and $4f_{5/2}$ bands occur at 84.0 and 87.7 eV, respectively, and are close to those expected for bulk gold. The Au 4f peaks are slightly asymmetric and could possibly contain two small peaks at 84.7 and 88.4 eV.[40] These additional peaks might be due to the distribution of particle size because a change in the Fermi level would be expected as the particle size is decreased. Alternatively, it could also indicate the presence of a thin oxide, or it could be due to surface charging. In the sulfur 2p region, we see two well-resolved peaks corresponding to the contributions of the $2p_{3/2}$ and $2p_{1/2}$ levels. These peaks occur at 162.1 and 163.4 eV, as would be expected for sulfur in the thiolate form.[41] The ratio of 2:1 found for $2p_{3/2}$ and $2p_{1/2}$ indicates that a single sulfur species is present. Mixed species tend to be "triangular" in shape because of the convolution of two or more doublets. Two peaks at were found in the C 1s region at 285 and 286 eV, respectively, corresponding to different carbon atoms in the heterocyclic aromatic ring. A N 1s peak was found at 399 eV as expected for this molecule. Both the S 2p and N 1s spectra suggest that it is the sulfur that is bonded to the gold and that there is no obvious interaction between nitrogen and gold. Details of peak positions and the relative amounts of the various chemical species present are listed in Table 4.

Figure 7 shows the XPS spectra of the 2MPm-modified nanoparticles. The Au 4f region is similar to that of the 2MPy nanoparticles. In addition to the two main peaks at 84.2 and 87.8 eV, two small peaks centered around 84.9 and 88.6 eV were found. The sulfur bands of the 2MPm nanoparticles are broader than those of the 2MPy nanoparticles, and three doublets

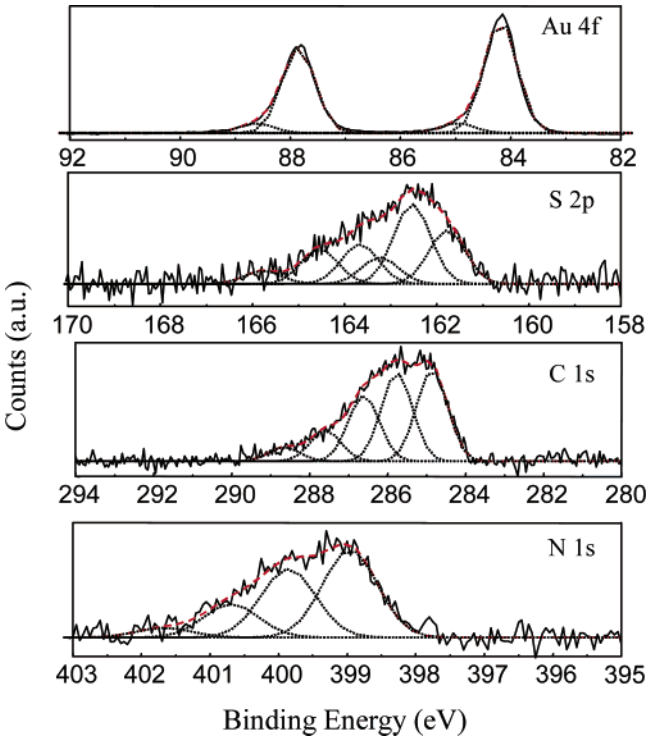

Figure 7. Au 4f, S 2p, C 1s, and N 1s regions of the XPS spectrum of 2MPm-passivated gold nanoparticles.

were used to fit the experimental data. The main contribution comes from the doublets with their S $2p_{3/2}$ bands at 161.8 and 162.5 eV, respectively (i.e., the thiolate). However, a weaker additional doublet, whose S $2p_{3/2}$ and S $2p_{1/2}$ levels are at 164.5 and 165.7 eV, respectively, was also detected at higher binding energy. Meanwhile, both the C 1s and N 1s peaks also contain a series of additional higher-binding-energy components. The reason for these additional peaks is not unambiguous, but it is possibly associated with a heterogeneous charge distribution within the sample or is due to a fraction of the 2MPm molecules not being bonded through the sulfur group and thus giving rise to a free thiol that is expected to have a higher binding energy. The nanoparticles have been carefully washed before being deposited onto silicon wafers so that the effects of excess organic materials in the sample can be ruled out. Hence, the additional peaks in Figure 7 seem to suggest that the 2MPm-passivated gold nanoparticles are easier to charge than the 2MPy particles. The different components in the C 1s and N 1s bands indicate different charging states in the samples and reveal a nonuniform charge distribution in thin films of the 2MPm nanoparticles. So far, we cannot conclude that surface charging is the only cause of the shifts; indeed, the IR spectra revealed that some 2MPm molecules adsorbed on the nanoparticles might remain

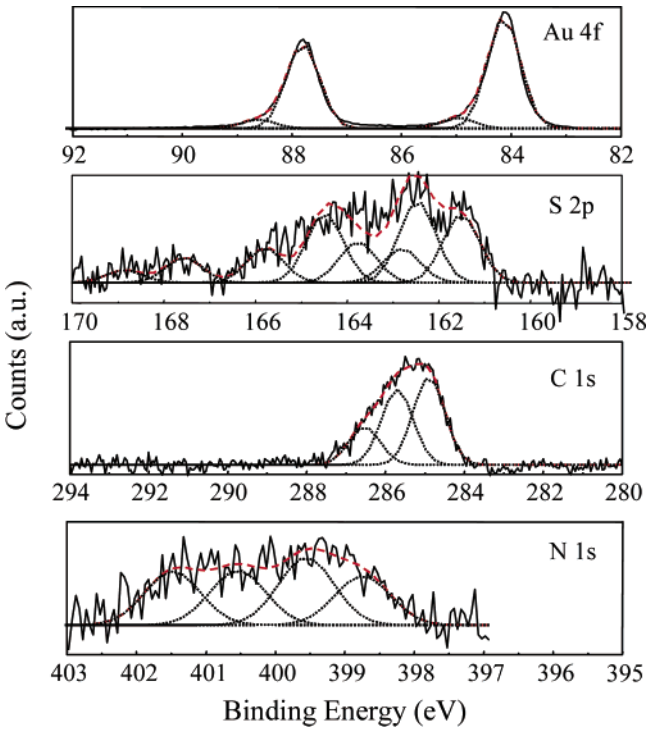

Figure 8. Au 4f, S 2p, C 1s, and N 1s regions of the XPS spectrum of 4MPy-passivated gold nanoparticles.

in the thione form, which may also contribute to the complexity of the spectra. Moreover, there has been SPM work showing that 2MPm could interact with Au(111) through both S and N atoms, which could also result in a shift of the XPS peaks. A complete understanding of this issue may require further theoretical and experimental effort.

The XPS spectra of the 4MPy-passivated gold nanoparticles are presented in Figure 8. The Au 4f bands of 2MPy nanoparticles show main peaks at 84.1 and 87.8 eV, similar to those of the 2MPy and 2MPm samples. Two small peaks were found around 85.0 and 88.6 eV having similar intensity to those in the 2MPy and 2MPm spectra. The S 2p of 4MPy nanoparticles shows a rather broad band indicating the coexistence of sulfur moieties in different chemical states. The analysis of the S 2p band suggests that there are at least four different sulfur species with their S $2p_{3/2}$ level varying from 161.5 to 167.6 eV. The sulfur species with the highest binding energy, whose S $2p_{3/2}$ and S $2p_{1/2}$ levels are at 167.6 and 168.9 eV, respectively, is possibly due to a small number of sulfone moieties, indicating some oxidization of the sulfur group in the 4MPy ligands. This reveals that some 4MPy molecules are adsorbed onto the gold surface through their nitrogen atoms, leaving sulfur groups free to oxidize. The C 1s peak is asymmetric and has multiple components; three peaks were fitted to the data at 284.9, 285.7, and 286.5 eV, respectively. The C 1s peak is less broad than that of the 2MPm samples, probably indicating less charging of the 4MPy nanoparticles. The N 1s band gives rise to four peaks between 398.8 and 401.5 eV. It is notable that the S 2p and N 1s bands in Figure 8 exhibit greater broadening than that seen for the C 1s peak, suggesting that these effects are more likely to be associated with surface binding of the 4MPy molecules to the gold surface.

Conclusions

This paper reports the first systematic investigation of the formation of gold nanoparticles passivated by the heterocyclic mercaptan derivatives 2MPy, 4MPy, and 2MPm. We have compared the feasibility of using these compounds as stabilizing ligands for nanoparticles. Among the three compounds, the 2MPy system gave the most stable and uniform nanoparticles. The 4MPy-passivated nanoparticles displayed a strong tendency to form 3D aggregates. We attribute the poor stability of the 4MPy functionalized nanoparticles to the cross linking between sulfur groups on neighboring particles. This arises from the bonding of a fraction of the 4MPy molecules through their nitrogen groups.

FTIR and UV−vis spectroscopy were employed to study the structural configuration of the heterocyclic molecules on the gold surface. Ab initio calculations of the vibrational spectra are in reasonable agreement with the observed spectra in the condensed phase, which therefore enables the assignment of the vibrational modes. Comparing the spectra of the molecules in KBr pellets with those of the nanoparticle samples shows that the thione form is predominant when the molecules are in a polycrystalline state, but the thiol-like form is observed for molecules adsorbed on the particles. However, UV−vis spectra show that traces of the thione form are detected in methanol solutions of 2MPy- and 2MPm-passivated nanoparticles and can possibly be attributed to the adsorption/desorption equilibrium of the ligands in solution. No 4MPy desorption is detected in the passivated nanoparticle solution. However, the plasmon band of 4MPy nanoparticles indicates a wide size distribution, consistent with the TEM finding that it forms 3D aggregates.

In XPS spectra of the 2MPy nanoparticles, the C 1s, S 2p, and N 1s peaks occur at positions close to those expected for these molecules, and no significant surface-charging effect is observed. In contrast, the peaks in the spectra of 2MPm- and 4MPy-passivated nanoparticles show dramatic shifts, possibly indicating that significant surface charging is present. Oxidization of the sulfur group is detected for 4MPy-modified nanoparticles, which could infer that some of the molecules are adsorbed onto the gold surface via nitrogen atoms.

This work reveals the complexity of using heterocyclic molecules to stabilize gold nanoparticles and highlights the need to understand the chemical properties of the ligand if we are to develop applications based on such particles. Investigations of the optical and electronic properties of the above nanoparticles assembled at various interfaces are currently underway in our group.

Acknowledgment. We acknowledge the EPSRC for financial support and for the use of the ESCA facility at the RUSTI laboratories, Daresbury, Warrington. We also thank Dr. R. Brydson for assistance with TEM measurements and Dr. J. Clarkson for his help in performing the ab initio calculations.

References and Notes

(1) Terrill, R. G.; Postlethwaite, T. A.; Chen, C.; Poon, C. D.; Terzis, A. Chen, A.; Hutchison, J. E.; Clark, M. R.; Wignal, G.; Londono, J. D.; Superfine, R.; Falvo, M.; Johnson, C. S., Jr.; Samulski, E. T.; Murray, R. W. *J. Am. Chem. Soc.* **1995**, *117*, 12537.

(2) Seshadri, R.; Subbanna, G. N.; Vijayakrishnan, V.; Kulkarni, G. U.; Ananthankrishna, G.; Rao, C. N. R. *J. Phys. Chem.* **1995**, *99*, 5639.

(3) Hostetler, M. J.; Stokes, J. J.; Murray, R. W. *Langmuir* **1996**, *12*, 3604.

(4) Shipway, A. N.; Katz, E.; Willner, I. *ChemPhysChem* **2000**, *1*, 18.

(5) Evans, S. D.; Johnson, S. R.; Cheng, Y. L.; Shen, T. *J. Mater. Chem.* **2000**, *10*, 183.

(6) Khlebtsov, N. G.; Bogatyrev, V. A.; Dykman, L. A.; Melnikov, A. G. *J. Colloid Interface Sci.* **1996**, *180*, 436.

(7) Connolly, S.; Cobbe, S.; Fitzmaurice, D. *J. Phys. Chem. B* **2001**, *105*, 2222.

(8) Weisbecker, C. S.; Merritt, M. V.; Whitesides, G. M. *Langmuir* **1996**, *12*, 3763.
(9) Bethell, D.; Brust, M.; Schiffrin, D. J.; Kiely, C. *J. Electroanal. Chem.* **1996**, *406*, 137.
(10) Johnson, S. R.; Evans, S. D.; Mahon, S. W.; Ulman, A. *Langmuir* **1997**, *13*, 51.
(11) Leff, D. V.; Ohara, P. C.; Heath, J. R.; Gelbart, W. M. *J. Phys. Chem.* **1995**, *99*, 7036.
(12) Brown, L. O.; Hutchison, J. E. *J. Am. Chem. Soc.* **1997**, *119*, 12384.
(13) Weare, W. W.; Reed, S. M.; Warner, M. G.; Hutchison, J. E. *J. Am. Chem. Soc.* **2000**, *122*, 12890.
(14) Sarathy, K. V.; Raina, G.; Yadav, R. T.; Kulkarni, G. U.; Rao, C. N. R. *J. Phys. Chem. B* **1997**, *101*, 9876.
(15) Cliffel, D. E.; Zamborini, F. P.; Gross, S. M.; Murray, R. W. *Langmuir* **2000**, *16*, 9699.
(16) Chen, S.; Kimura, K. *Langmuir* **1999**, *15*, 1075.
(17) Khlebtsoy, N.; Bogatyrev, V. A.; Dykman, L. A.; Melnikov, A. G. *J. Colloid Interface Sci.* **1996**, *180*, 436.
(18) Novak, J. P.; Brousseau, L. C.; Vance, F. W.; Johnson, R. C.; Lemon, B. I.; Hupp, J. T.; Feldheim, D. L. *J. Am. Chem. Soc.* **2000**, *122*, 12029.
(19) Johnson, S. R.; Evans, S. D.; Brydson, R. *Langmuir* **1998**, *14*, 6639.
(20) Elguero, J.; Marzin, C.; Katritzky, A. R.; Linda, P. *The Tautomerism of Heterocycles*. Advances in Heterocyclic Chemistry; Academic Press: New York, 1976; Supplement 1.
(21) Stoyanov, S.; Petkov, I.; Antonov, L.; Stoyanova, T.; Karagiannidis, P.; Aslanidis, P. *Can. J. Chem.* **1990**, *68*, 1482.
(22) Penfold, B. R. *Acta Crystallogr.* **1953**, *6*, 707.
(23) Zhang, H. L.; Chen, M.; Li, H. L. *J. Phys. Chem. B* **2000**, *104*, 28.
(24) Alonso, C.; Pascual, M. J.; Salomon, A. B.; Abruna, H. D.; Gutierez, A.; Lopez, M. F.; Garcia-Alonso, M. C.; Escudero, M. L. *J. Electronanal. Chem.* **1997**, *435*, 241.
(25) Taniguchi, I.; Yoshimoto, S.; Yoshida, M.; Kobayashi, S.; Miyawaki, T.; Aono, Y.; Sunatsuki, Y.; Taira, H. *Electrochim. Acta* **2000**, *45*, 2843.
(26) Lamp, B. D.; Hobara, D.; Poter, M. D.; Niki, K.; Cotton, T. M. *Langmuir* **1997**, *13*, 736.
(27) Zhang, H.; He, H. X.; Wang, J.; Liu, Z. F. *Langmuir* **2000**, *16*, 4554.
(28) Sawaguchi, T.; Mizutani, F.; Yochimoto, S.; Taniguchi, I. *Electrochim. Acta* **2000**, *45*, 2861.
(29) Pinheiro, L. S.; Temperini, M. L. A. *Appl. Surf. Sci.* **2001**, *171*, 89.
(30) Baldwin, J. A.; Vlckva, B.; Andrew, M. P.; Butler, I. S. *Langmuir* **1997**, *13*, 374.
(31) Pang, J. S.; Hwang, H. J.; Kim, M. S. *J. Mol. Struct.* **1998**, *441*, 63.
(32) Zhang, Z.; Imae, T. *J. Colloid Interface Sci.* **2001**, *233*, 99.
(33) Frisch, M. J.; Trucks, G. W.; Schlegel, H. B.; Scuseria, G. E.; Robb, M. A.; Cheeseman, J. R.; Zakrzewski, V. G.; Montgomery, J. A., Jr.; Stratmann, R. E.; Burant, J. C.; Dapprich, S.; Millam, J. M.; Daniels, A. D.; Kudin, K. N.; Strain, M. C.; Farkas, O.; Tomasi, J.; Barone, V.; Cossi, M.; Cammi, R.; Mennucci, B.; Pomelli, C.; Adamo, C.; Clifford, S.; Ochterski, J.; Petersson, G. A.; Ayala, P. Y.; Cui, Q.; Morokuma, K.; Malick, D. K.; Rabuck, A. D.; Raghavachari, K.; Foresman, J. B.; Cioslowski, J.; Ortiz, J. V.; Stefanov, B. B.; Liu, G.; Liashenko, A.; Piskorz, P.; Komaromi, I.; Gomperts, R.; Martin, R. L.; Fox, D. J.; Keith, T.; Al-Laham, M. A.; Peng, C. Y.; Nanayakkara, A.; Gonzalez, C.; Challacombe, M.; Gill, P. M. W.; Johnson, B. G.; Chen, W.; Wong, M. W.; Andres, J. L.; Head-Gordon, M.; Replogle, E. S.; Pople, J. A. *Gaussian 98*, revision A.5; Gaussian, Inc.: Pittsburgh, PA, 1998.
(34) Foresman, J. B.; Frisch, A. *Exploring Chemistry with Electronic Structure Methods*, 2nd ed.; Gaussian, Inc.: Pittsburgh, PA, 1996.
(35) Szymanski, H. A. *Interpreted Infrared Spectra*; Plenum Press: New York, 1964; Vol. 1, pp 80, 81.
(36) In the following discussion, the term "thiol-like form" is used to describe the molecule that adopts a form that has similar electronic structure to its thiol tautomer. It does not necessarily mean that there is still a hydrogen remaining on the sulfur group. Similarly, the term "thione-like form" is used to describe the molecule that adopts a form that has similar electronic structure to its thione tautomer.
(37) Contreras, J. G.; Seguel, G. V.; Alderete, J. B. *Spectrochim. Acta* **1994**, *50*, 371.
(38) Nowak, M. J.; Rostkowska, H.; Lapinski, L. *Spectrochim. Acta* **1991**, *47*, 339−353.
(39) Raj, C. R.; Kitamura, F.; Ohsaka, T. *Langmuir* **2001**, *17*, 7378−7386.
(40) The Au 4f spectra were fitted using a peak width of 0.7 eV, whereas for all of the other spectra a width of 0.8 eV was used.
(41) Beamson, G.; Briggs, D. *High-Resolution XPS of Organic Polymers*; The Scienta ESCA300 Database; Wiley & Sons: Chichester, U.K., 1992.